Natural Hazards and Earth System Sciences (2001) 1: 53–59

Natural Hazards and Earth System Sciences

Comparison of simultaneous variations of the ionospheric total electron content and geomagnetic field associated with strong earthquakes

Sh. Naaman[1], **L. S. Alperovich**[1], **Sh. Wdowinski**[1], **M. Hayakawa**[2], **and E. Calais**[3]

[1]Dept. of Geophysics and Planetary Sciences, Tel-Aviv University, PO Box 39040, Ramat Aviv, Israel
[2]Dept. of Electronic Engineering, University of Electro-Communications, 1-5-1 Chofugaoka, Chofu Tokyo 182-8585, Japan
[3]Central National De La Recherche Scientifique, Universite De Nice-Sophia Antipolis, Geosciences Azur, Valbone, France

Received: 15 May 2001 – Revised: 3 July 2001 – Accepted: 18 July 2001

Abstract. In this paper, perturbations of the ionospheric Total Electron Content (TEC) are compared with geomagnetic oscillations. Comparison is made for a few selected periods, some during earthquakes in California and Japan and others at quiet periods in Israel and California. Anomalies in TEC were extracted using Global Positioning System (GPS) observations collected by GIL (GPS in Israel) and the California permanent GPS networks. Geomagnetic data were collected in some regions where geomagnetic observatories and the GPS network overlaps. Sensitivity of the GPS method and basic wave characteristics of the ionospheric TEC perturbations are discussed. We study temporal variations of ionospheric TEC structures with highest reasonable spatial resolution around 50 km. Our results show no detectable TEC disturbances caused by right-lateral strike-slip earthquakes with minor vertical displacement. However, geomagnetic observations obtained at two observatories located in the epicenter zone of a strong dip-slip earthquake (Kyuchu, $M = 6.2$, 26 March 1997) revealed geomagnetic disturbances occurred 6–7 h before the earthquake.

1 Introduction

The purpose of this paper is to study (1) capability of GPS measurements as a tool for solid Earth-ionosphere coupling, (2) sensitivity and accuracy of the ionospheric GPS observations and finally (3) to present some case studies with ionospheric Total Electron Content (TEC) and geomagnetic interrelations. We combine both ionospheric and geomagnetic observations in order to detect a precursor prior to earthquakes.

Correspondence to: L. S. Alperovich
(leonid@frodo.tau.ac.il)

2 Sensitivity of ionospheric measurements using GPS observations

GPS is an all-weather, spaced-based radio navigation system, designed and maintained by the U. S. Department of Defence (DoD) for military and civilian purposes. The GPS satellite constellation contains six polar orbits, close to circular with semimajor axis of 26 000 km and period of slightly less then 12 h (Dixon, 1991). The GPS provides 24-h 3-dimensional positioning and timing. The system uses 28 satellites that have been operated since 1980 by the US DoD. At any given time and location around the globe, a GPS receiver has at least 6 GPS satellites in sight.

GPS satellites transmit electromagnetic waves for positioning on two frequencies: L1 (1.57542 GHz) and L2 (1.2276 GHz). The velocity of an electromagnetic wave at the GHz band is frequency dependent in the ionosphere. This enables us to extract the ionospheric TEC along the line of sight, satellite-receiver. The absolute TEC, calculated using GPS is given by (Manucci et al., 1993).

$$TEC = \frac{\Delta\rho \cdot c}{40.3} \cdot \frac{f_1^2 \cdot f_2^2}{f_1^2 - f_2^2} \quad (1)$$

where TEC is Total Electron content (el/m^2), $\Delta\rho$ (m) is the distance equal to light velocity c (m/s) multiplied by the difference between time delays measured by the L1 and L2 wave packet, f_1 is the frequency of the L1 wave and f_2 is the second frequency (L2 wave).

In order to estimate the sensitivity of the ionospheric GPS method of TEC observations and obtain basic wave characteristics of the TEC perturbations in the ionosphere, calibration of GPS receivers was performed using several permanent stations with various distances between them. For near-zero base line we use two receivers located 50 m apart, Fig. 1a demonstrates the dependency of TEC on time for

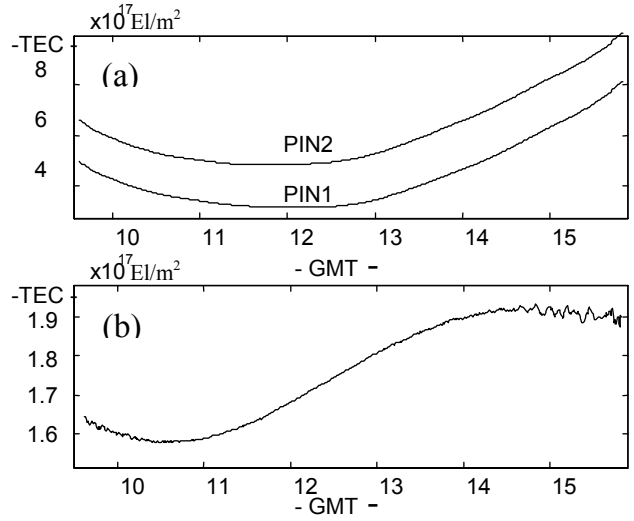

Fig. 1. **(a)** Ionospheric TEC [electrons/m^2] calculated using observations by two receivers (PIN1, PIN2) located 50 m from one another. **(b)** The difference in TEC measurements between the two receivers as a function of time.

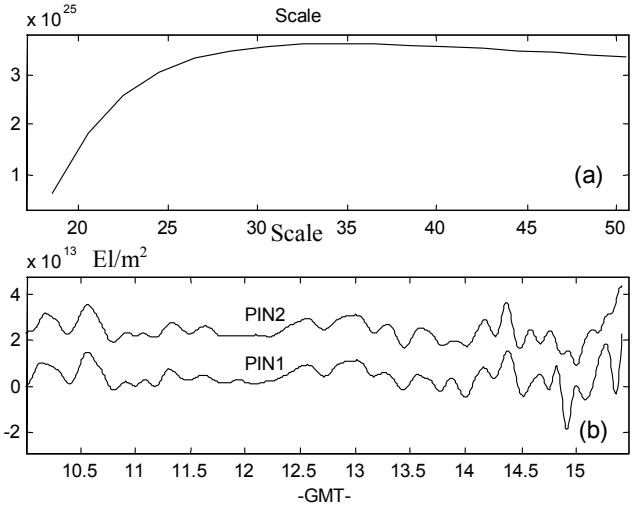

Fig. 2. **(a)** Example of the scale dependency of the cross-correlation function between two signals obtained using two receivers at the near zero base line. Maximum correlation is obtained at 36 min, **(b)** Decomposed signal using the Mexican-hat wavelet (scale=36-min). The offset between the two decomposed signals obtained from PIN1 and PIN2 is arbitrary only for demonstration.

those two receivers. The natural TEC gradient between such points should be zero; any unmatched measurements are associated with receiver noise or multipath effects. Those two receivers are part of the California permanent GPS network and the data obtained from Scripps Institution of Oceanography (SIO).

Typically, daily TEC variation ranges from 10^{16} el/m^2 (night conditions) to 10^{18} el/m^2 (daylight conditions). Comparison at near-zero baseline (Fig. 1b) shows an artificial average difference of $1.8{\cdot}10^{17}$ el/m^2 and another sinusoidal-like difference with amplitude of $3{\cdot}10^{16}$ el/m^2 and high frequency noise at the beginning and end of the observations. Observations, using data transmitted by other satellites, show that the sinusoidal-like TEC difference changes independently for each satellite, indicating environmental independent errors (temperature, humidity, etc.), Lanyi and Roth (1988) explained this distinction as P-code offsets and multipath effects. High frequency deviations appear at low elevation angle, at the beginning and the end of observation session, when the satellite rises and sets. This high frequency noise is due to ionospheric effects, which are more pronounced at low elevation where the signal passes through a thick ionospheric layer.

We applied a continuous wavelet transform method (based on the 'Mexican hat' testing function) and calculated the correlation function for the TEC-series of both receivers in the range of 2–50 min. The maximum likeness was found at 36 min scale (Fig. 2a). For a scale smaller then 25 min the correlation function decreases sharply indicating high frequency noise. For scales larger than 36 min, the correlation function decreases slowly monotonically. Figure 2b demonstrates the decomposed signal from those two receivers using The Mexican-hat wavelet (scale=36-min). A comparison TEC recorded between small distances demonstrates the ultimate in relative coincidence with an accuracy of 10^{13} el/m^2 for quiet conditions, which is around 0.1% of the observed TEC (Fig. 2b).

This calibration has been used for the study of small ionospheric variations. Ionospheric sequences of earthquakes have been examined based on data from the Southern California Integrated GPS Network and two GPS receivers located in Japan. The Israeli GPS network has been used for sensitivity tests.

GPS in Israel (GIL). GIL is a network of 10 permanent receivers operated and maintained by Tel Aviv University (TAU), Survey of Israel (SOI) and the Israel Space Agency. Distances between sites vary from 30 to 400 km and around 8 satellites are visible simultaneously with the array. An observation from one satellite (PRN 24) was collected using five receivers; TEC was determined using 30 s sampling rate. Discrete wavelet decomposition was applied on the GPS signal based on the Mexican hat wavelet scale at 36 min. The result is presented in Fig. 4.

In order to estimate the sensitivity of the ionospheric GPS method in determining of TEC observations and to obtain basic wave characteristics of the ionospheric perturbations, a coherency analysis was conducted for two Israeli GPS receivers located at distances from 50 m to 200 km. A comparison between TEC recorded at small distances demonstrates the agreement with an accuracy of 10^{14} el/m^2; this value is around of 1% of the regular TEC. Data analyses of two remote receivers revealed several travelling ionospheric disturbances (TID). The TID observed with the GPS system were mostly of short duration with 2–3 oscillations. Therefore, usual Fourier analysis is not appropriate, and the following

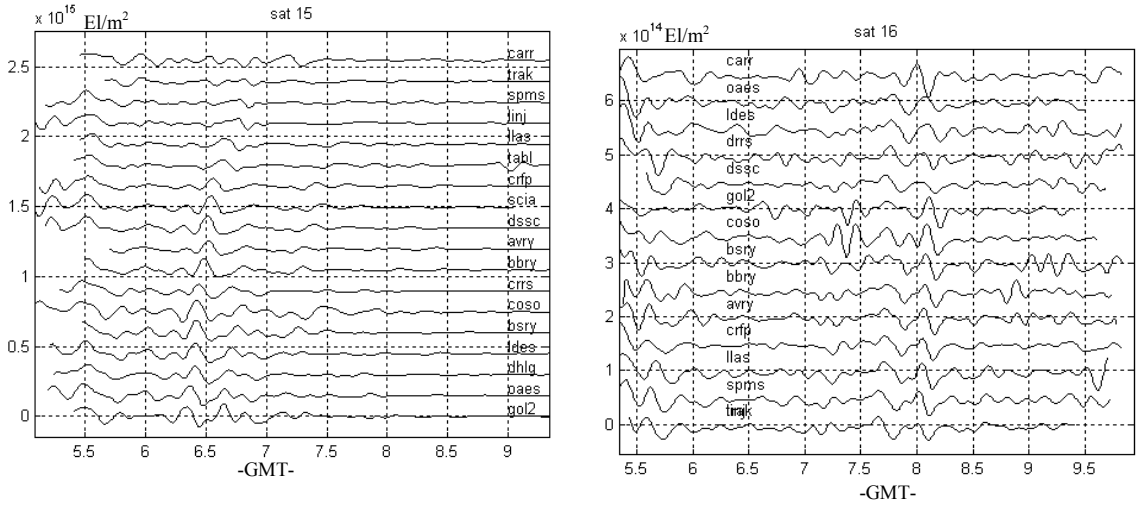

Fig. 3. (a) Observation from satellite number 15; the travelling ionospheric disturbance (TID) can be seen as a wave shifted with time at each site. **(b)** Observation from satellite 16; the same TID observed by satellite 15 but with reduced amplitude occurring one and a half-hour later.

procedure was adopted.

We first determined TEC for a 30 s sampling and then performed discrete and continuous wavelet decompositions of the GPS signal based on a short wavelet. Generating a series of TEC maps provides a convenient method for choosing between alternative interpretations of observed TID. We tried to detect disturbances with velocities of more than 20 km/min. If we extract such waves we should find every reason to explain them in terms of the slow hydromagnetic waves "loaded by neutrals" and propagating in the partially ionised ionospheric plasma (Piddington, 1955; Sorokin and Fedorovich, 1982; Alperovich and Zheludev, 1997). In general, we attribute the main wave background of TEC disturbances to regular acoustic and acoustic-gravity waves. However providing an explanation for the TID is beyond the scope of this paper.

The methodology outlined in this section for tracing of a TID is simple and robust. We examine filtered time-series of ionospheric TEC obtained by different receiver- satellite pairs. We compute the projection of a satellite-receiver line to the 300 km height for each visible satellite. Then we compare time-delays between maxima of the same wave trains as seen by each satellite-receiver pairs. Knowing the time-delay and the relative distance between the respective points on the reference height (300 km) enables us to define the horizontal velocity of a TID. Figure 5 shows results of the satellite trajectory mapping onto the reference level (300 km). Asterisks represent the location of the receiver.

3 GPS and geomagnetic measurements prior two strong earthquakes

Southern California Integrated GPS Network (SCIGN). SCIGN provides continues regional coverage of GPS observations throughout Southern California. The network contains more than two hundred stations.

We examined TEC data obtained from SCIGN network during the 16 October 1999 M7.1 Hector Mine Earthquake, which occurred at 10:46 GMT. Because the earthquake was right-lateral strike-slip with minor vertical displacement, we did not expect to obtain any ionospheric reaction. Indeed, checking the three satellite observations taken by the BBRY site during the day of the Hector Mine earthquake yielded no significant ionospheric response that could be related to the earthquake.

Data from October determined the TID that originated from an eastward zone and moved from the northeast to the southwest, with velocity of 10 km/min across the epicentral zone (Figs. 3a and b). We used observations from two satellites and several SCIGN selected sites. All selected sites observed the variation in the signal of satellite 15 at 6:30 GMT (Fig. 3a). The shifts of the TID maximum and the distance between sites provide the information regarding the direction and velocity of TID propagation. The same TID, recognizeable by its shape, was observed by satellite 16 one and a half-hours after satellite 15 s observations. The signal amplitude was reduced from $2.5{\cdot}10^{14}$ el/m^2 for the first observation to $0.5{\cdot}10^{14}$ el/m^2 for the second observation.

Study of TEC during the 17 January 1994 Northridge, CA earthquake, which was blind thrust displacement, shows ionospheric response as a wave with frequency and phase velocities that are consistent with acoustic-gravity waves excited by seismic source (Calais and Minster, 1995). These results confirm the hypothesis for acoustic-gravity waves as an efficient link between solid Earth-atmosphere-ionosphere.

Japan 1997. We tailor our wavelet methods to ensure that an earthquake produced TID actually exists in the TEC wave perturbations. We study data from two Japanese GPS receivers (tskb: 36.1° N, 140° E; usud: 36.1° N, 138° E) after and before two strong earthquakes ($M = 6.2$, 26 March

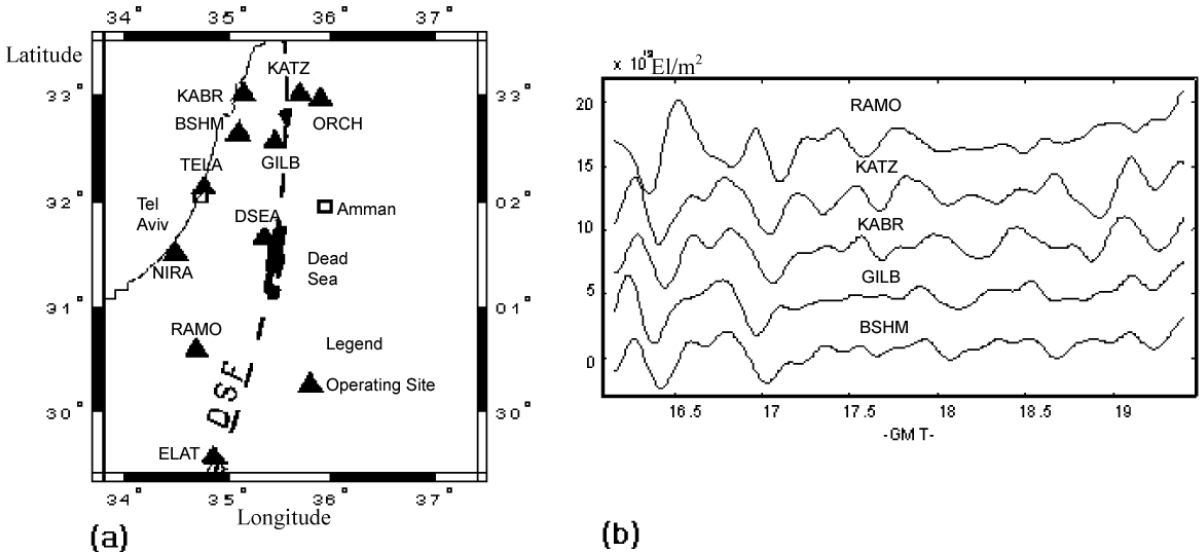

Fig. 4. (a) Map of the GIL network **(b)** Decomposition of TEC observations obtained from one satellite at five GIL receivers. The similarity of the signal at the KATZ, KABR, GILB and BSHM sites, which are located between 30–60 km apart, is obvious. In contrast, the RAMO site is located 240 km from these and shows a different signal.

1997/08:31 GMT, 32.0° N, 130.3° E; $M = 6.1$, 13 May 1997/14:35 GMT, 31.9° N, 130.3° E).

Five satellites were observed using the TSKB receiver (Fig. 6a). The ionospheric TEC obtained from this receiver and geomagnetic time series obtained by two magnetometers located at Kanoya (31.48° N, 130.72° E) and Kagosima (31.42° N, 130.98° E), (Fig. 6a) show that no simple relation can be found between ionospheric and geomagnetic variations. Since the correspondence between ground geomagnetic perturbations and the TEC variations has not been examined so far, more detailed analyses for both geomagnetic and ionospheric data are needed to separate magnetospheric, ionospheric and geotectonic-related anomalies.

Figure 7 shows filtered magnetograms obtained at Kanoya (Figs. 7c and d) and Kagoshima (Figs. 7a and b) observatories at 26 March 1997. The filtration was obtained using the wavelet 'Mexican hat' with 50 s scale. Strong magnetic pulse is seen at 00:57 UT and at 01:53 UT at Kagoshima magnetometer. The same pulse reduced in amplitude and shifted in time is seen in the Kanoya magnetogramas.

4 Discussion and conclusions

Analysis of GPS data from the dense California Integrated GPS Network revealed background 10–15 min wave trains propagating with velocity of 10 km/min. Consequently, TID has been revealed and traced with intensity of $10^{13} - 10^{14}$ el/m^2. The average value of the coherency radius of the TEC disturbances is $\approx$ 50–100 km.

A reverse faulting earthquake demonstrates ionospheric response to earthquake. The main contribution to the TEC is from a region with maximum electron density of about 300 km. Otherwise; small atmospheric disturbances reaching these heights can be transformed into shock waves (Romanova, 1975). Thus, the GPS method, based on phase measurements, works quite well with atmospheric energy releases associated with large-scale atmospheric perturbations. An earthquake with strong vertical displacement of the Earth's surface can produce plane waves in the neutral atmosphere propagating upward. Study of the TEC during the 17 January 1994, Northridge, CA earthquake, which was reverse faulting, shows ionospheric response (Calais et al., 1998). The signal amplitude was $\approx 10^{14}$ el/m^2.

We also examined ionospheric disturbances, around the time of the strong Californian earthquake ($M = 7.1$, Hector Mine earthquake), with lateral tectonic motion but without essential large-scale vertical motions. GPS observations do not show any anomaly associated with the quake.

Perturbations of the vertical electric field, if they occurred, could cause ionospheric anomalies but only in the D-layer (Alperovich and Fedorov, 1998) and the impact on the TEC is insignificant. Careful examination of the TEC based on the wavelet technique and comparison of filtered data of different simultaneous GPS selected sites, has not reveal any TEC perturbations (running away) from the ionosphere above the epicenter zone preceding an earthquake.

On the other hand, geomagnetic observations obtained at two observatories, located essentially in the epicenter zone and spaced 25 km apart, have revealed two successive pulses 6–7 h ahead of the earthquake in Kyuchu ($M = 6.2$, 26 March 1997). However, geomagnetic observations preceding another earthquake, with the epicenter in the same place (Kyuchu, $M = 6.2$, 13 May 1997), have not demonstrated any detectable anomalies.

The reason why the pulses were not observed during the second earthquake, which occurred in the same place, may

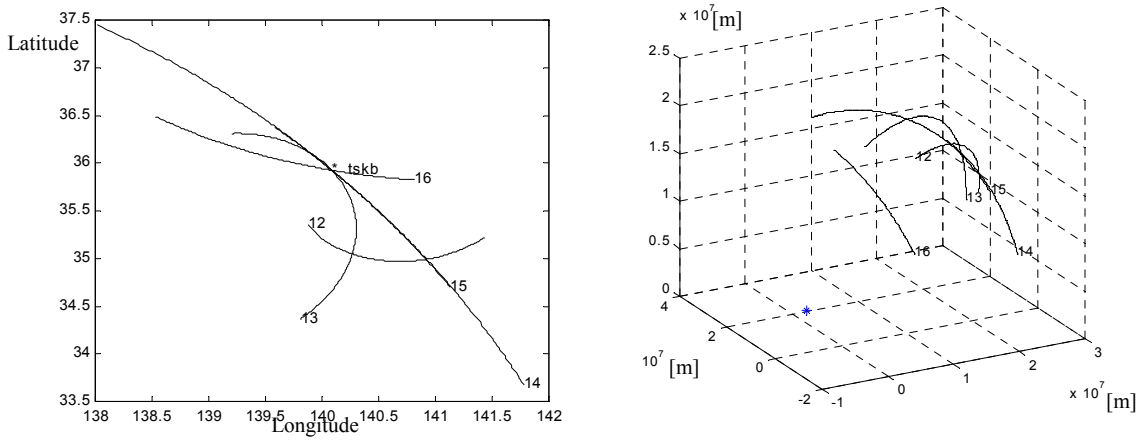

Fig. 5. Satellite trajectory at the ionospheric level. The number of each satellite is located at the point of the first observation location.

be due to their distinct depths. The hypocenter of the first quake was at a depth of 30 km and the second at 16 km. At first glance it might be thought that the second should also generate the same pulses. Moreover, due to the proximity to the ground surface, the magnetic signal should be of high intensity. This is incorrect since the both earthquake sources are centered in regions with essentially different conductivity. There is a deep minimum of geoelectrical resistivity, at a depth of 15–20 km, reaching tens of Ohm·m in 'hot' areas with intensive heat fluxes (or in a zone with high tectonic activity) (Vanyan, 1997). In contrast, the depth of 30–50 km is characterized by the high resistivity of hundreds of Ohm·m.

Leaving aside the question of generation of such impulses (Gershenzon and Gohberg, 1994; Molchanov and Hayakawa, 1998) the availability or lack of magnetic pulses can in principle be explained by propagation conditions. The source of the second quake is located in the high conductive layer surrounded by the low conductive medium. On the other hand, the situation of the first earthquake is a low conductive waveguide with high conductive walls. An electromagnetic wave can propagate here as a 'diffusive' wave with low velocity and high damping.

Wavelet analysis of Kagoshima and Kanoya magnetic records yielded, at both sites, two successive pulses of the same shape with 3.2 min and 6.8 min time delays, respectively. The distance between the two observation points is about 25 km. Hence, we estimate the horizontal wave velocities of the pulses as 8 km/min and 4 km/min. Figure 7 also shows that the intensity of the pulses is strongly dependent on the distance. It follows, from the Fig. 7, that the attenuation rate α is 0.1 km^{-1}.

The pulses manifest themselves predominantly in the H-component. Taking into account the relative locations of the observation points and the epicentre of the first quake, one can see that the wave propagated from the epicentre via Kagoshima to Kanoya with a strong longitudinal magnetic component. Let us consider the damping coefficient α for an H-wave propagating in the waveguide with rectangular cross-section of sides a and b. For the magnetic-type wave $H_{n1,n2}(n_1, n_2 \neq 1)$ we have (Landau and Lifshitz, 1984).

$$\alpha = \frac{2c\kappa^2\zeta}{\omega k_z ab}\left[a + b + \frac{k_z^2}{k^4}\left(k_x^2 a + k_y^2 b\right)\right] \quad (2)$$

where $k_x = n_1\pi/a$, $k_y = n_2\pi/b$, k_z are the wave numbers along the waveguide axis, $\kappa^2 = \omega^2/c^2 - k_z^2$, c is the speed of light, and ζ is the surface impedance of the surrounded media

$$\left(\zeta = (1-i)\sqrt{\omega/8\pi\sigma}\right).$$

Here, σ is the specific conductivity (s^{-1}). Let for simplicity neglect second and third terms. Then

$$\alpha = 2c\kappa^2\zeta/(\omega k_z b) \approx 2c\zeta k_z/(\omega b)$$

and for thickness of the waveguide we have

$$b \approx 2c\zeta k_z/(\alpha\omega) \approx ck_z/\left(\alpha\sqrt{2\pi\sigma\omega}\right).$$

Assuming that the horizontal velocity of the wave is $\approx$ 10 km/min, the oscillation period is of $\approx$ 1 min; then the wave number $k_z = 0.6\,\mathrm{km}^{-1}$. The conductivity of the walls is $5{\cdot}10^8\,s^{-1}$ (Vanyan, 1997). We find that $b \approx 100$ km.

We conclude that the observed characteristics of the impulse can be interpreted merely as a result of propagation of the electromagnetic wave in a waveguide of about 100 km thickness.

Confirmation, that the discovered impulses are natural and non man-made, was given by thorough wavelet analysis of magnetograms for half the 1997 year at both the Kagoshima and the Kanoya observatories. We tried to find impulses, as discussed above, appearing simultaneously at these sites to exclude the artificial interference field source. These impulses are unique in this sense.

It appears reasonable that, among the remaining local disturbances, there are industrial electromagnetic noise and impulses produced by an earthquake. We developed and tested (Alperovich et al., 2001) a robust algorithm based on the

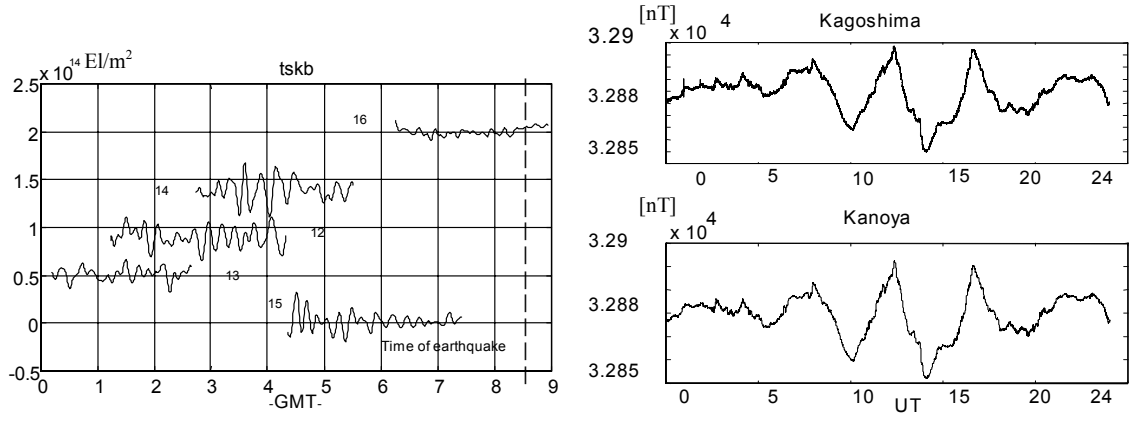

Fig. 6. a, b: Geomagnetic and ionospheric time series before the earthquake at Kyuchu on 26 March 1997.

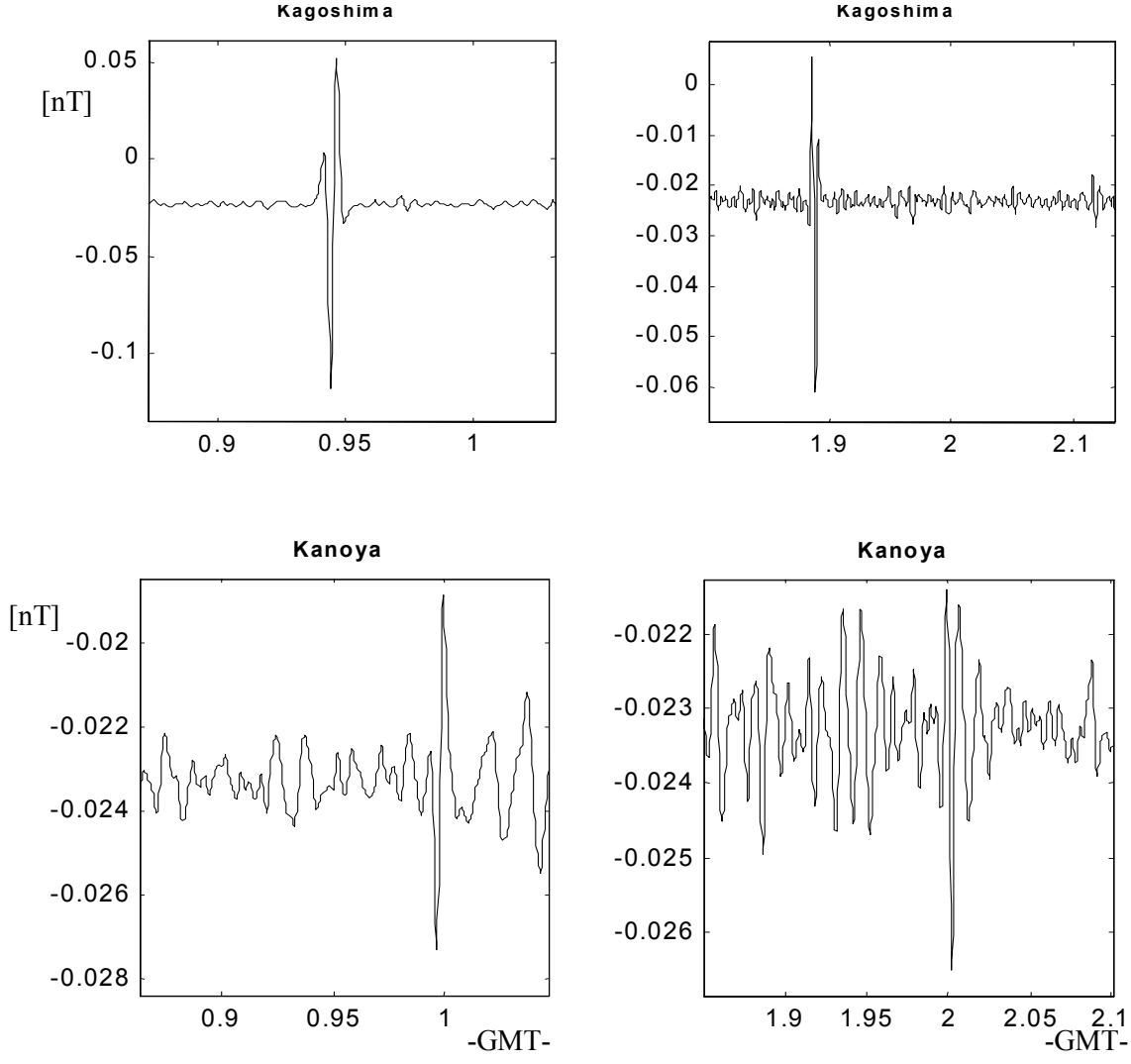

Fig. 7. Two sequenced pulses observed simultaneously by the Kagoshima and Kanoya observatories at 26 March 1997. The time delay between the first pulse fixed by the both observatories is 3.2 min, and for the second pulse is 6.8 min. The distance between the two observation points is about 25 km. Thus, the horizontal velocities are ≈ 8 km/min and ≈ 4 km/min.

wavelet approach that solves two related problems: (1) Classification of geomagnetic signals produced by underground and magnetospheric sources. (2) Detection of the presence of earthquake-caused signals in the ground-based magnetograms. We have analyzed 0.5-year records of the geomagnetic pulsations at Kagoshima and all earthquakes in a radius from 50 to 1000 km with their center in Kagoshima. It has been found that there is specific class of short 1-min wave trains preceding earthquakes in the 100 km radius. From the results of these tests and the analysis outlined above, we conclude that the strong localized magnetic surges should be considered as a geomagnetic signature of an underground seismic source.

In summary, we believe that joint geomagnetic—TEC analysis can illuminate potential pitfalls in methods for retrieval of ionospheric and electromagnetic disturbances associated with an earthquake. Such observations may lead to the development of a new approach to avoid these pitfalls and take full advantage of the electromagnetic methods of earthquake predictions.

Acknowledgements. We acknowledge the Southern California Integrated GPS Network and its sponsors, the W. M. Keck Foundation, NASA, NSF, USGS, SCEC, for the data of the California GPS network. The geomagnetic data of Kagoshima observatory were kindly provided by Prof. K. Yumoto and the members of the 210° MM team (Yumoto et al., 1992). The authors gratefully acknowledge the useful discussion with Prof. O. Molchanov.

References

Alperovich, L. and Zheludev, V. A.: Global fast and slow ELF waves as deduced from the multistationed low- and sub-auroral geomagnetic measurements, Adv. Space Res., 20, 513–516, 1997.

Alperovich, L. and Fedorov, E.: Perturbation of atmospheric conductivity as a cause of the seismo-inospheric interaction, Phys. Chem. Earth, 23, 945–947, 1998.

Alperovich, L., Zheludev, V., and Hayakawa, M.: Comparative wavelet study of long-period geomagnetic variations associated with the 1989 $M = 7.1$ Loma Prieta and two 1997 $M = 6.1$ Japanese earthquakes, IWSE 3rd monograph, 2001.

Calais, E., Minster, J. B., Hofton, M. A., and Hedlin, M. A. H.: Ionospheric signature of surface mine blasts from Global Positioning System measurements, Geophys. J. Int., 132, 191–202, 1998.

Calais, E. and Minster, J. B.: GPS detection of ionospheric perturbations following the 17 January 1994, Northridge earthquake, Geophys. Res. Lett., 22, 1045–1048, 1995.

Dixon, T. H.: An introduction to the Global Positioning System and some geological applications, Rev. Geophys., 29, 249–276, 1991.

Gershenzon, N. I. and Gohberg, M. B.: On the origin of anomalous ultralow-frequency geomagnetic disturbances prior to Loma Prieta, California, earthquake, Physics of the Solid Earth, 30, 112–118, 1994.

Landau, L. D. and Lifshitz, E. M.: Electrodynamics of continuos media, (Eds) Lifshitz, E. M. and Pitaevskii, L. P., 2nd Edition, Pergamon Press, pp. 460, 1984.

Lanyi, G. E. and Roth, T.: A comparison of napped and measured total ionospheric content using the Global Positioning System and Beacon satellite observations, Radio Sci., 23, 483–492, 1988.

Manucci, A. J., Wilson, B. D., and Edwards, C. D.: A new method for monitoring the Earth's ionospheric total electron content using the GPS global network, presented at ION GPS-93, Salt Lake City, 22–24 September 1993.

Molchanov, O. A. and Hayakawa, M.: On the generation mechanism of ULF seismogenic electromagnetic emissions, Phys. Earth and Planet. Int., 105, 201–210, 1998.

Piddington, J. H.: Hydromagnetic waves in ionized gas, Monthly Notices of Roy. Astr. Soc., 115, 671, 1955.

Romanova, N. N.: Vertical propagation of acoustic waves of arbitrary shape in the isothermal atmosphere, Izvestia ANSSSR (fizika atmosphere oklana), 11, 233–242, 1975.

Sorokin, V. M. and Fedorovich, G. V.: The Physics of the Slow-Waves in the Ionosphere. Moscow, Energoizdat, 1982.

Vanyan, L. L.: Electromagnetic soundings, Moscow (in Russian), Nauchnyi MIR, pp. 218, 1997.

Yumoto, K., Tanaka, Y., Oguti, T., Shiokawa, K., Yoshimura, Y., Isono, A., Fraser, B. J., Menk, F. W., Lynn, J. W., and Seto, M.: Globally coordinated magnetic observations along 210-degrees magnetic meridian during step period, 1: Preliminary results of low-latitudes Pc3S, Journ. Geomagn. Geoelectr., 44, 261–276, 1992.